CSCE Annual Conference

Growing with youth – Croître avec les jeunes

Laval (Greater Montreal)

June 12 - 15, 2019

SHOULD WE CONSIDER THE PLASTIC CAPACITY OF STRUCTURAL SYSTEMS IN THE DESIGN OF WIND-EXCITED BUILDINGS? A CRITICAL EXAMINATION OF DAMAGE ACCUMULATION, DUCTILITY DEMAND, AND HYSTERETIC ENERGY

Bezabeh, Matiyas[1,2,3], Bitsuamlak, Girma[1], Tesfamariam, Solomon[2]
[1] Western University, Canada
[2] University of British Columbia-Okanagan, Canada
[3] matiyas.bezabeh@alumni.ubc.ca

Abstract: The lateral strength and stiffness requirements due to wind loads usually govern the design of tall buildings. The current building codes in the U.S.A, Canada, and Europe recognize the first significant yield point as an ultimate limit state. The main argument used in favor of linear-elastic design approach is its presumed ability to avoid unidirectional yielding and the subsequent damage accumulation due to the longer duration of wind storms. Consequently, the current design practices ignore the plastic capacity of structural systems in the nonlinear range, which could result in uneconomical and brittle buildings. Thus, in this paper, we re-examined the classical linear-elastic design arguments with consideration of performance-based wind engineering approaches, innovative technologies, and materials. As the first step towards PBWE, this paper has demonstrated the benefits of considering the nonlinear capacity of structural systems in the design of wind-excited buildings. In all, we have postulated, then proved, the capability of self-centering systems in controlling the possible damage accumulation in structural systems subjected to long-duration wind loads. Our arguments are based on an extensive parametric study through nonlinear time history analyses considering peak and residual ductility-demands, normalized hysteretic energy dissipation, and the rate of damage accumulation as performance indicators. Overall, the results of the study revealed that self-centering systems could benefit the most from the "*ductility-based*" design due to their inherent re-centering capability, higher energy dissipation, and their less sensitivity to wind duration.

1 INTRODUCTION

The architectural and structural forms of the recent generation of tall buildings show a trend towards complex bluff geometry, reduced weight, stiffness, and damping, leading to an increased excitation by the wind. Therefore, the lateral strength and stiffness requirements due to wind load usually govern the design of tall buildings. Currently, tall buildings are being designed by only considering the linear-elastic behavior of structural systems. The existing building codes and standards such as NBCC-2015 and ASCE 7-10 (ASCE 2010) consider the first significant yield point as an ultimate limit state, which could result in uneconomical (overdesigned) and brittle buildings. This implies that the current design process of tall buildings is not sensible when considering the safety and the economics of owners and society.

The main argument used in favor of linear-elastic design approach is its presumed ability to avoid unidirectional yielding and the subsequent damage accumulation due to the longer duration of wind storms. For a given building, the notion of the current design approach expects the predicted design wind loads to be, on average, lower than the yield capacity of the structural systems (Davenport 1975). Therefore, the

wind response of tall buildings beyond their design capacity is not accurately known. Even though the inherent ductility of materials could give some extra time for evacuation, a non-ductile building subjected to long duration wind load could collapse in the brittle mode of failure. Plastic deformations of tall buildings under tropical cyclones and tornadoes are reported in Davenport (1975). For example, the structural damages to the 18-story Meyer-Kiser tall steel building during the Great Miami Hurricane of 1926, which sustained 1-minute average wind speed of ~45m/s for more than 1 hour, resulted in a significant amount of accumulated residual drift. Due to the severity of the accumulated damage, right after the hurricane, the Meyer-Kiser building was shortened to 7-story. The case of Mayer-Kiser building indicates that linear-elastic design approaches *per se* do not guarantee safe and economical structures.

As seen in earthquake engineering, a philosophically consistent extension of the current wind design approach is, therefore, "*ductility-based design*" or "*performance-based design*." This shift in paradigm, however, requires new performance objectives (such as "controlled damage" and "collapse prevention"), analysis methods such as nonlinear static pushover and nonlinear time history analysis under wind loads, and mechanisms to control damage accumulation. In wind engineering, suggestions to design structures for different performance objectives (limit states) was first introduced by Davenport (1975). The identified limit states in Davenport (1975) are the collapse to the mainframe due to excessive permanent drift, damage to architectural finishes, excessive acceleration (occupant discomfort), and integrity of cladding and finishing materials.

The studies towards the performance-based wind engineering (PBWE) can be categorized into two broad research directions. The first group of studies focused on the response of simple yielding structural systems subjected to turbulent wind loads (e.g., Vickery 1970, Chen and Davenport 2000, Hong 2004, Gani and Légeron 2012). Overall, these studies highlighted the importance of considering the damage accumulation and ductility-capacity in wind design. The second research direction has focused on the development of a comprehensive PBWE frameworks, to name a few, Ciampoli et al. 2011, Griffis et al. 2013, Mohammadi 2016, Spence et al. 2016, Elezaby 2017, Cui and Caracoglia 2018, Bezabeh et al. 2018b). Most of the existing PBWE frameworks focused on extending the earthquake engineering methodology into wind engineering. These formulations are essential in developing the roadmap towards complete PBWE. However, they may suffer from the lack of accuracy due to the inherent differences between earthquake and wind loads, primarily in load duration, frequency content, and damage mechanisms.

In general, without controlling the residual displacement, which can accumulate and trigger a brittle collapse of the mainframe, performance-based wind design of buildings may not be safe and economical. In our opinion, the first step in PBWE, therefore, should be understanding the response of structures in the non-linear range and control damage accumulation. Thus, in this paper, we critically examined the ductility-demand, the effect of wind duration, hysteretic energy, and the rate of damage accumulation using nonlinear time history analysis of Single-Degree-of-Freedom (SDOF) systems. We proposed the use of self-centering systems and proved their capability in controlling the possible damage accumulation in structural systems subjected to long-duration wind loads.

2 OVERVIEW OF SELF-CENTERING LOAD RESISTING SYSTEMS

Recently, several numerical, analytical, and experimental studies show that with the use of various types of self-centering systems, the possibility of reducing and, in some cases, eliminating residual displacements (e.g., Aiken et al. 1993, Priestley et al. 1999, Ganey et al. 2017). Apart from the development of mechanically driven self-centering (SC) systems, few researchers investigated the potential application of Shape Memory Alloys (SMAs) to reduce or eliminate residual deformations. SMAs are a type of smart materials that can develop "*shape memory*" and "*superelastic (pseudo-elastic)*" behaviors by phase transformation that can be initiated either by stress or temperature. DesRoches et al. (2004) reported the minimal effect of size on the super-elasticity of SMA bars. This was an important finding that justifies the application of superelastic SMA for large scale civil structural systems. Recently, few researchers explored the potential application of SMA to reduce seismically induced damages. Saiidi and Wang (2006) and Alam

et al. (2009) explored the potential benefits of SMA based reinforcement bars in RC structures subjected to seismic loads.

3 NONLINEAR DYNAMIC ANALYSIS OF STRUCTURES UNDER WIND LOADS

In this section, we briefly define the basic terminologies, discuss the hysteretic models and analysis procedures for nonlinear dynamic analysis of structures under wind loads.

3.1 The equation of motion and generation of artificial fluctuating wind speed time series

The equation of motion of a SDOF system under wind load is given in Eq. 1.

$$[1] \quad m\ddot{x} + c\dot{x} + f_r(x, \dot{x}) = F_w(t)$$

where $m\ddot{x}$ is the inertial force of the system, $c\dot{x}$ is the damping force, $f_r(x, \dot{x})$ is the restoring force as a function of displacement (x) and velocity ($\dot{x}$) responses. The time varying wind force, $F_w(t)$, acting on the system can be determined from Eq. 2, by assuming a direct correlation between wind fluctuations on the structure and the upstream (Quasi-Steady theory, Davenport 1961).

$$[2] \quad F_w(t) = \frac{1}{2}\rho C_d A[V + v(t)]^2$$

In Eq. 2, ρ is air density, A is exposed area of SDOF system, C_d is the drag coefficient, V is the mean wind speed, and $v(t)$ is the fluctuating wind speed. We targeted the Davenport spectrum (Davenport 1961) to generate artificial wind speed time series using the spectral representation method (Shinozuka and Jan 1972). In Davenport (1961) it is shown that the power spectral density (PSD) of the along wind speed is:

$$[3] \quad \frac{fS(z,f)}{u_*^2} = 4\frac{(1200f/V(10))^2}{(1 + (1200f/V(10))^2)^{4/3}}$$

where f is the frequency in Hz, $S(z,f)$ PSD at height z, u_* is shear friction velocity, which is $V(z)k/(ln\, z/z_o)$, z_o is the roughness length of the upstream fetch whose value is dependent on the terrain condition. According to the spectral method, the fluctuating wind speed time series is:

$$[4] \quad v(t) = \sqrt{2}\sum_{j=1}^{n}\sqrt{S(z,f_j)\Delta f}\cos(2\pi f_j + \theta_j)$$

where f_j is a frequency point within the range 0 and f_{max} spaced at a constant interval (Δf), θ_j is random phase angle uniformly distributed between 0 and 2π. In this paper, the maximum frequency, f_{max} is set at 5 Hz considering the significant decay of turbulent gust energy beyond 1 Hz. Simulations with a sampling frequency of 10 Hz are suitable to perform dynamic structural analysis in the time domain. To avoid unintended periodicity, we kept n greater than the number of time steps. For demonstration, samples of the simulated time histories and corresponding average spectra are depicted in Fig. 1. The parameters of the demonstration simulation are $z = 10m$, $z_o = 0.05$, and $V(10) = 30\ m/s$. Fig. 1 shows a good agreement between the target Davenport spectrum and the average PSD of two artificially generated wind speed times series data.

The evaluation of structural responses using Eq. 1 requires idealization of the restoring force, $f_r(x, \dot{x})$ to represent "*realistic*" structural systems. In this study, we considered four idealized force-deformation (hysteresis) models, i.e., linear-elastic (Fig. 2a), elastic-plastic (Fig. 2b), bilinear (Fig. 2c), and self-centering (flag shaped, Fig. 2d). As shown in Fig. 2, the considered models can be completely defined by initial stiffness (k), yield strength demand (F_y), post-yield stiffness ratio (α), and energy dissipation capacity (β).

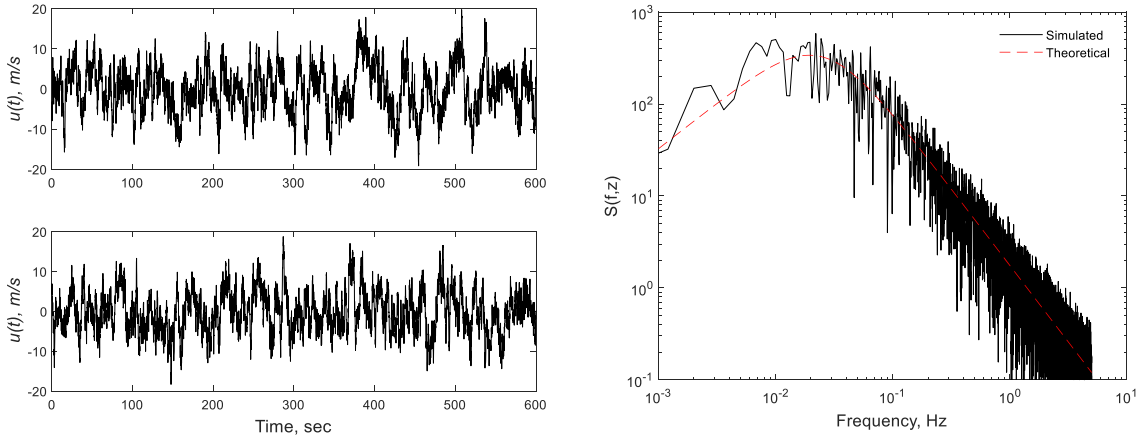

a) b)

Fig. 1: Generation of artificial fluctuating wind speed time series: a) simulated wind speed time series; b) comparison of mean PSD of simulated wind time series and the target theoretical Davenport spectrum

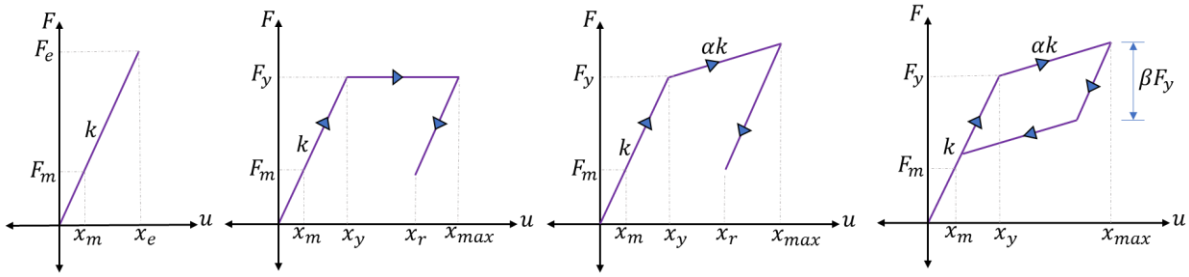

a) b) c) d)

Fig. 2: Hysteretic models considered in the study: a) linear-elastic; b) elastic-plastic; c) bilinear; d) self-centering (flag-shaped)

In Fig. 2, (F_m, x_m) are coordinates of the mean along-wind force and the corresponding displacement, (F_y, x_y) are the coordinates of the yield force and the corresponding yield displacement, and (F_e, x_e) are coordinates representing the linear-elastic factored design wind load and design displacements, respectively. In addition, x_{max} and x_r are the maximum and residual displacements of the nonlinear system without considering shake down, respectively.

3.2 Demand and capacity parameters

If a structural system is designed in such a way that its yield strength (F_y) is less than the elastic design force F_e, then the system responds inelastically (excursions towards nonlinear response range occur). Deformation performance of systems in the nonlinear response range can be described by the ductility demand (μ).

[5] $$\mu = \frac{x_I}{x_y}$$

where x_I is displacement response greater than or equal to yield displacement x_y. In earthquake engineering, it is customarily to use the observed peak ductility demand $\mu_{max} = x_{max}/x_y$ and residual ductility demand $\mu_{res} = x_{res}/x_y$ as performance indicators.

In general, nonlinear response characterization can be carried out by adjusting the mean wind speed (also the mean wind load, F_m) with respect to the yield strength (F_y). Even though this ratio does not include the fluctuation component of the wind loads in an explicit manner, one may choose it to perform initial response characterization and sensitivity study. In this paper, we named this factor as a *force modification factor (M)*. As the name implies, this factor controls the level of wind excitation with respect to the system yield capacity.

[6] $$M = \frac{F_m}{F_y}$$

As mentioned earlier, unidirectional excursions towards inelastic range due to the presence of mean wind load results in a significant amount of residual displacement (permanent set). Due to this distinct response behavior of structural systems under wind load, most of the cumulative damage demand parameters developed for earthquake engineering applications may not be suitable. For a lightly damped system, Vickery (1970) considered damage rate per crossing as a performance indicator and developed closed-form analytical expressions. Chen and Davenport (2000) also adopted the same parameter to study the inelastic response of structural systems under wind loads. In this paper, we considered the normalized damage rate per each zero-crossing (d_{acc}) as a damage accumulation index.

[7] $$d_{acc} = \frac{x_{res} - x_y}{\nu_0 T \sigma_x}$$

Hysteretic energy is another important cumulative damage parameter (performance indicator) that relates the amount of dissipated energy with the frequency and magnitudes of nonlinear excursions. This parameter can be estimated from the energy balance law. This can be achieved by introducing instantaneous displacement to the equation of motion (Eq. 1) and integrating over the whole wind duration as follows:

[8] $$\int_0^T m\ddot{x}\dot{x}dt + \int_0^T c\dot{x}^2 dt + \int_0^T f_r(x,\dot{x})\dot{x}dt = \int_0^T F_w(t)\dot{x}dt$$

In Eq. 8, $\int_0^T m\ddot{x}\dot{x}dt$ is a temporary kinetic energy of the SDOF system, $\int_0^T c\dot{x}^2 dt$ is the energy dissipated through damping, $\int_0^T f_r(x,\dot{x})\dot{x}dt$ is the total absorbed hysteretic energy which is the summation of irrecoverable hysteretic energy (plastic strain energy) and recoverable strain energy (elastic strain energy), and $\int_0^T F_w(t)\dot{x}dt$ the total input energy from the wind load. Usually, the total absorbed energy is normalized to include the effect of system stiffness and strength. The normalized hysteretic energy is:

[9] $$NHE = \frac{\int_0^T f_r(x,\dot{x})\dot{x}dt}{F_y x_y}$$

In this paper, we shall use Newmark's average acceleration Beta-algorithm (Newmark 1962, Chopra 2000) to solve Eq. 1. To account for the change of stiffness and damping with time in the nonlinear range, tangent-stiffness proportional Rayleigh damping approach is implemented.

3.3 Nonlinear response SDOF systems under wind loads

In the analyses, both bilinear and SC SDOF systems are characterized by a fundamental frequency f_n = 0.3 Hz, post-yield stiffness ratio α = 3%, damping ratio ξ = 1%, and hysteretic energy dissipation β = 0.6. To generate $v(t)$, we assumed the mean wind velocity V = 30m/s, turbulence intensity I_u = 18.75%, height the SDOF systems z = 10m, wind duration T = 600 sec. We added 100 seconds of additional zero wind

loads at the end of each time history to allow the systems to achieve a new equilibrium state through a damped free vibration. We varied the level of wind excitation to the system capacity, *M*, between 0.1 to 0.9.

Fig. 3 compares the ductility time histories of the bilinear (*black line*) and SC (*red line*) SDOF systems under one artificially generated wind load time history. It is apparent from the figure that ductility-demand (μ) increases with *M* for both hysteretic models. When *M* is less than 0.3, the responses are within the linear-elastic range. A significant amount of nonlinear response is observed in both systems as *M* increases beyond 0.4. Irrespective of *M*, it is shown that μ of SC systems is always less than the corresponding bilinear systems. Fig. 3 depicts the unbounded growth of μ of bilinear systems with time, resulting in an exceptionally large residual displacement that could either trigger collapse or need uneconomical repair after the excitation. For all considered excitation to capacity level, SC systems completely return to their initial position without incurring any residual displacement. Figs. 4 and 5 show the normalized force-ductility curves of bilinear and SC systems, respectively. Again, μ increases with M for both SDOF systems. The hysteretic responses of the bilinear systems (Fig. 4) are dominated by elastic-unloading and elastic-reloading where the system could not form stable hysteretic loops due to the presence of the static mean wind load. Moreover, as shown in Fig. 4, when bilinear systems modeled considering M greater than 0.7, the first excursion in to the nonlinear range results in a large plastic deformation.

On the contrary, Fig. 5 shows the ability of self-centering systems in controlling permanent displacement. Moreover, the systems respond with stable cyclic loops with distinctive hysteretic energy dissipative region. Figs. 6a and 6b show the peak-ductility (μ_{max}) and residual-ductility (μ_{res}) demand curves of bilinear SDOF systems, respectively. The responses are extracted from the results of 250 independent nonlinear time history analyses (NLTHA). Each curve of μ_{max} and μ_{res} versus *M* in Fig. 6 is the result of a dynamic analysis under one wind load time history. In the figures, to clearly show the dispersions, we provided statistical summary curves (10%, 50%, and 90% fractile curves). As expected both μ_{max} and μ_{res}, in bilinear systems, are strongly correlated and monotonically increase with M. Moreover, as can be seen from the figures, due to the presence of the mean wind load (the inability of the system to re-center), μ_{max} and μ_{res} are almost the same order of magnitude.

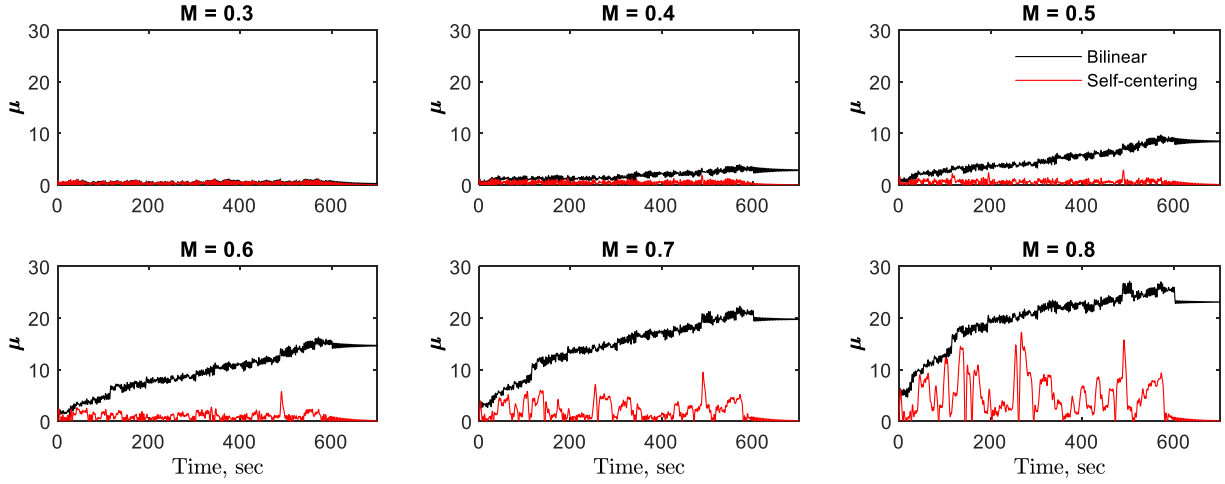

Fig. 3: Nonlinear time history responses of bilinear (black line) and SC (red line) for various levels of M

Fig. 7a shows the μ_{max} curves of SC SDOF systems. Inspection of the obtained results show that, for all levels of *M*, the median μ_{max} of the bilinear system is higher than the SC system. However, the dispersion of the response curves is higher in SC systems than the bilinear systems (Fig. 6a and 7a). In Fig. 7b, we plotted the probability density function (PDF) of μ_{max} of SC systems to show the level of response uncertainty with respect to *M*. As shown in the figure, as *M* increases the uncertainty μ_{max} increases, which is marked by the widened and fattened PDFs. Using Eq. 7, to investigate how damage grows with the number of plastic excursions, we quantified the normalized damage rate per crossing (d_{acc}) of bilinear systems. This parameter is not quantified for SC systems, as they do not incur any permanent displacement

or damage. The results are presented in Fig. 8a. The variation of d_{acc} with *M* is more uncertain than both μ_{max} and μ_{res}. Moreover, when *M* exceeds 0.7, d_{acc} becomes less sensitive to *M*, which is marked by the flattening of the response curves. Similar trends of d_{acc} of bilinear systems are reported in Hong (2004). For design and post-disaster mitigation purposes, it is common to develop prediction equations of the residual displacements as a function of peak response parameters. Hence, to visualize the relationship between the peak and residual displacements, we computed the normalized rate of damage accumulation based on the peak inelastic displacement as $d_{acc}(peak) = (x_{max} - x_y)/vT\sigma_x$ and plotted it against d_{acc} in Fig. 8b. As expected, $d_{acc}(peak)$ is always higher than d_{acc}. The figure also shows that if *M* < 0.7, a linear relationship holds between the d_{acc} and $d_{acc}(peak)$, otherwise, the results scatter.

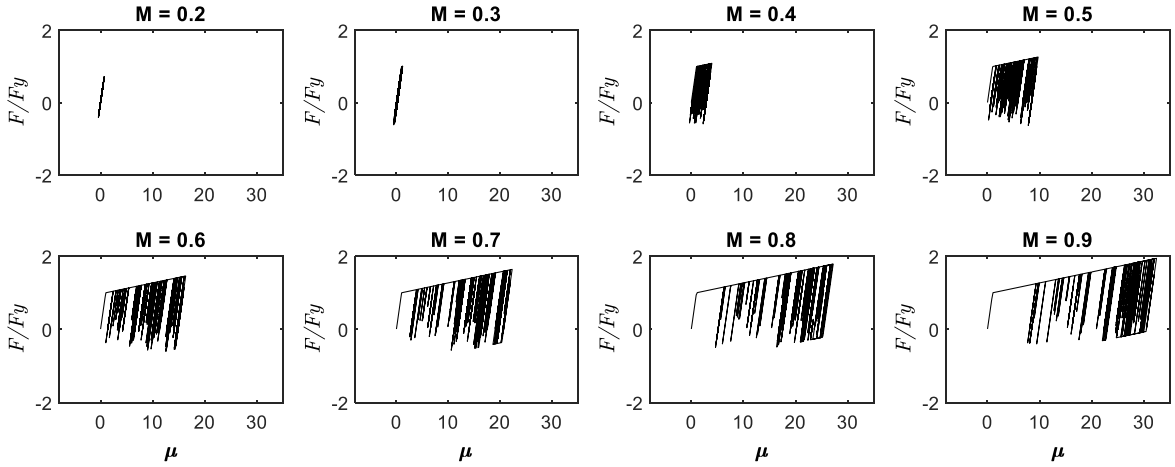

Fig. 4: Normalized internal force-deformation response curves of bilinear systems

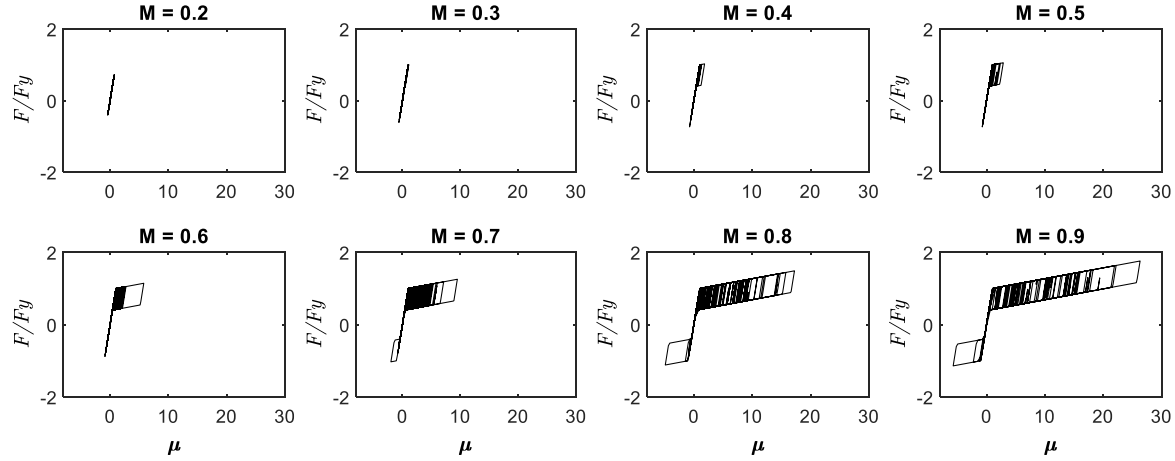

Fig. 5: Normalized internal force-deformation response curves of SC systems

Fig. 9 compares the energy dissipation capacity of bilinear and SC systems when subjected to a single wind load time history. When comparing the *NHE* of these systems at *M* = 0.3 – 0.5, both bilinear and SC systems dissipated a comparable amount of energy throughout the whole duration of the wind load. However, at higher values of *M*, SC systems dissipate more energy than bilinear systems. This phenomenon can be better described by studying the force-deformation responses presented in Figs. 4 and 5.

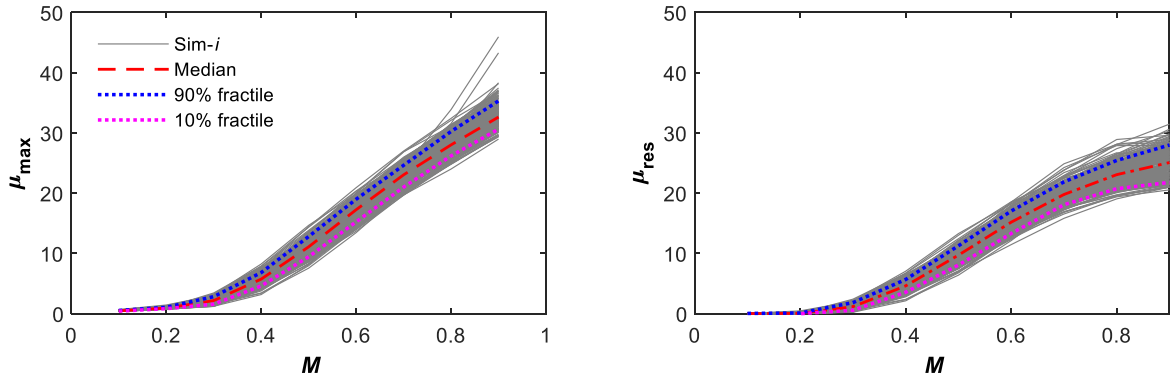

a) b)

Fig. 6: Ductility-demand curves of bilinear SDOF systems: a) peak; b) residual

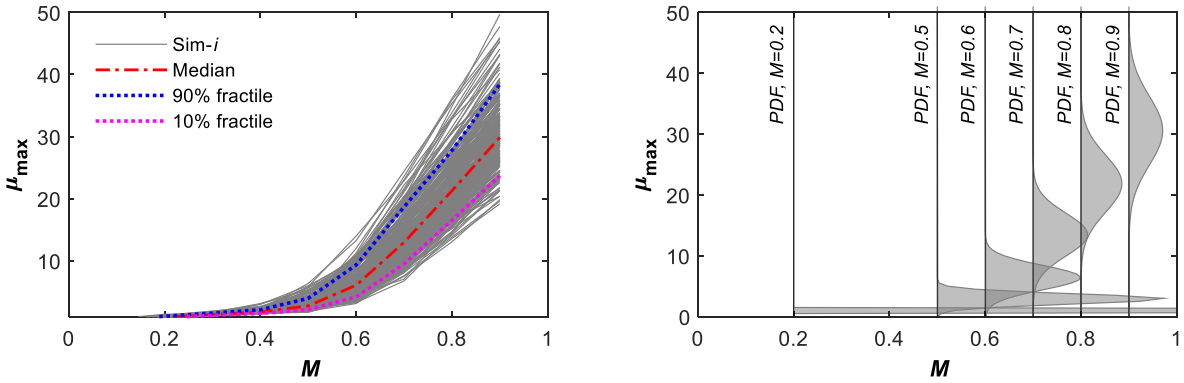

a) b)

Fig. 7: a) peak ductility-demands of SC systems; b) variation of PDF of peak ductility demand with M

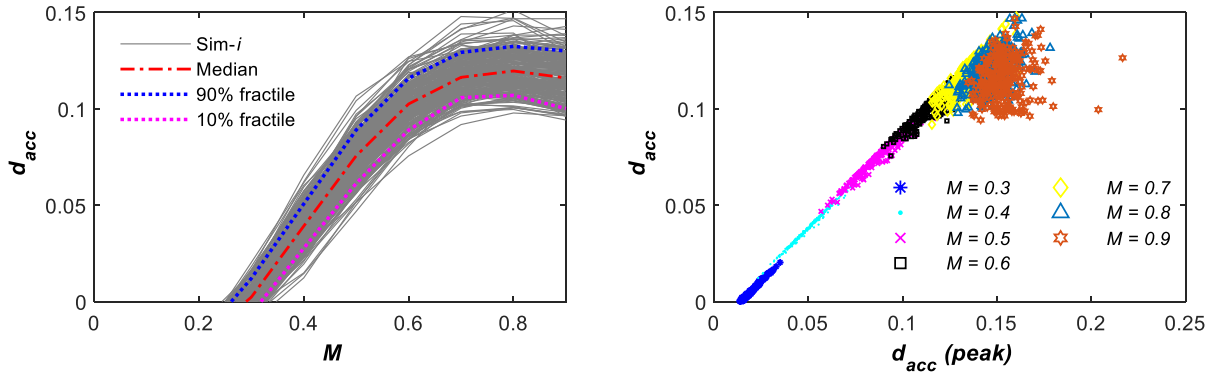

a) b)

Fig. 8: a) rate of damage accumulation in bilinear systems; b) scatter plot of $d_{acc}(peak)$ versus d_{acc}

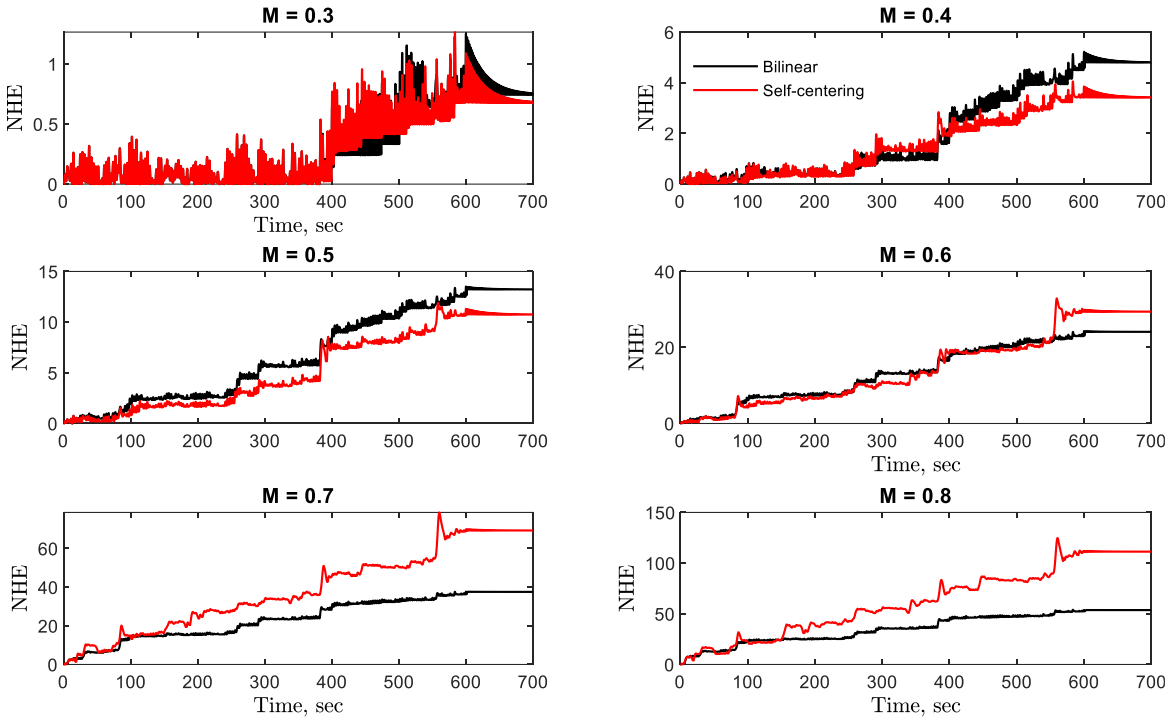

Fig. 9: Comparison of NHE time history between the bilinear system (black line) and SC system (red line) for various levels of M

4 SUMMARY AND CONCLUSIONS

As the first step towards PBWE, this paper has demonstrated the benefits of considering the nonlinear capacity of structural systems in the design of wind-excited buildings. In all, we have postulated, then proved, the capability of self-centering systems in controlling the possible damage accumulation in structural systems subjected to long-duration wind loads. Our arguments are based on an extensive parametric study through NLTHA considering peak and residual ductility-demands, normalized hysteretic energy dissipation, and the rate of damage accumulation as performance indicators. For the assumed structural and wind load simulation parameters, the major conclusions from the NLTHA are:

- For both bilinear and SC SDOF systems, ductility-demand (μ) is always directly proportional to the ratio of mean wind force to yield capacity, *M*. In bilinear systems, μ grows unboundedly with time, resulting in an exceptionally large residual displacement that could either trigger collapse or require uneconomical repair after the excitation.

- The hysteretic response of the bilinear systems is dominated by elastic-unloading and elastic-reloading, where the system could not form stable hysteretic loops due to the presence of the static mean wind load. The variation of d_{acc} in bilinear systems with *M* is more uncertain than both μ_{max} and μ_{res}. Moreover, when *M* exceeds 0.7, d_{acc} becomes less sensitive to *M*, which is marked by the flattening of the response curves.

- As expected, for all considered *M* values, self-centering systems completely return to their initial position without incurring any residual displacement (permanent set). Irrespective of *M*, it is shown that μ of SC systems is always less than the corresponding bilinear systems.

- Even with the presence of the mean part in the along-wind loads, SC systems always respond with a distinct energy dissipation region. At higher values of M, SC systems dissipate more energy than bilinear systems.

5 REFERENES

Aiken, I. D., Nims, D. K., Whittaker A.S. and Kelly, J. M. (1993). Testing of passive energy dissipation systems. Earthquake Spectra. Vol. 9, no. 3, pp. 335-370.

Alam, M. S., Nehdi, M., & Youssef, M. A. (2009). Seismic performance of concrete frame structures reinforced with superelastic shape memory alloys. Smart Struct Syst, 5(5), 565-585.

Bezabeh, M. A., Bitsuamlak, G. T., Popovski, M., & Tesfamariam, S. (2018b). Probabilistic serviceability-performance assessment of tall mass-timber buildings subjected to stochastic wind loads: Part II-structural reliability analysis. Journal of Wind Engineering and Industrial Aerodynamics, 181, 112-125.

Chen, D., & Davenport, A. G. (2000). Vulnerability of tall buildings in typhoons. Advances in Structural Dynamics, 2, 1455-1462.

Cui, W., & Caracoglia, L. (2015). Simulation and analysis of intervention costs due to wind-induced damage on tall buildings. Engineering Structures, 87, 183-197.

Davenport, A. G. (1961). A statistical approach to the treatment of wind loading on tall masts and suspension bridges. Ph.D. Dissertation, University of Bristol, United Kingdom.

Davenport, A. G. (1975). Tall buildings-an anatomy of wind risks. Construction in South Africa.

DesRoches, R., McCormick, J., & Delemont, M. (2004). Cyclic properties of superelastic shape memory alloy wires and bars. Journal of Structural Engineering, 130(1), 38-46.

Elezaby, F. Y. (2017). A performance based design approach for tall buildings under wind loading. Masters Thesis, Western University, Canada.

Gani, F., & Légeron, F. (2012). Relationship between specified ductility and strength demand reduction for single degree-of-freedom systems under extreme wind events. Journal of Wind Engineering and Industrial Aerodynamics, 109, 31-45.

Ganey, R., Berman, J., Akbas, T., Loftus, S., Daniel Dolan, J., Sause, R., Ricles, J., Pei, S., van de Lindt, J., Blomgren, H. E. (2017). Experimental Investigation of Self-Centering Cross-Laminated Timber Walls. Journal of Structural Engineering, 143(10), 04017135.

Griffis, L., Patel, V., Muthukumar, S., & Baldava, S. (2013). A framework for performance-based wind engineering. In Advances in Hurricane Engineering: Learning from Our Past (pp. 1205-1216).

Hong, H. P. (2004). Accumulation of wind induced damage on bilinear SDOF systems. Wind and Structures, 7(3), 145-158.

Mohammadi, A. (2016). Wind Performance Based Design for High-Rise Buildings. Ph.D. Dissertation, Florida International University, U.S.A.

Priestley, M. N., Sritharan, S., Conley, J. R., & Pampanin, S. (1999). Preliminary results and conclusions from the PRESSS five-story precast concrete test building. PCI journal, 44(6), 42-67.

Saiidi, M. S., & Wang, H. (2006). Exploratory study of seismic response of concrete columns with shape memory alloys reinforcement. ACI Structural Journal, 103(3), 436.

Shinozuka, M., & Jan, C. M. (1972). Digital simulation of random processes and its applications. Journal of sound and vibration, 25(1), 111-128.

Spence, S. M. J., Chuang, W. C., Tabbuso, P., Bernardini, E., Kareem, A., Palizzolo, L., & Pirrotta, A. (2016). Performance-Based Engineering of Wind-Excited Structures: A General Methodology. In Geotechnical and Structural Engineering Congress 2016 (pp. 1269-1282), USA.

Vickery, B. J. (1970). Wind action on simple yielding structures. Journal of the Engineering Mechanics Division, 96(2), 107-120.